Astronomy Letters, Vol. 29, No. 7, 2003, pp. 437–446. Translated from Pis'ma v Astronomicheskiĭ Zhurnal, Vol. 29, No. 7, 2003, pp. 497–507.

The Shape of the Rotation Curves of Edge-on Galaxies

A. V. Zasov[1]* and A. V. Khoperskov[2]

[1] *Sternberg Astronomical Institute, Universitetski pr. 13, Moscow, 119992 Russia*

[2] *Volgograd State University, Department of Theoretical Physics, Volgograd, 400068 Russia*

Received February 4, 2003

Abstract—We consider the effects of projection, internal absorption, and gas or stellar velocity dispersion on the measured rotation curves of galaxies with edge-on disks. Axisymmetric disk models clearly show that the rotation velocity in the inner galaxy is highly underestimated. As a result, an extended portion that imitates nearly rigid rotation appears. At galactocentric distances where the absorption is low (i.e., it does not exceed 0.3–0.5^m kpc^{-1}), the line profiles can have two peaks, and a rotation curve with minimum distortions can be obtained by estimating the position of the peak that corresponds to a higher rotation velocity. However, the high-velocity peak disappears in high-absorption regions and the actual shape of the rotation curve cannot be reproduced from line-of-sight velocity estimates. In general, the optical rotation curves for edge-on galaxies are of little use in reconstructing the mass distribution in the inner regions, particularly for galaxies with a steep velocity gradient in the central region. In this case, estimating the rotation velocities for outer (transparent) disk regions yields correct results. © *2003 MAIK "Nauka/Interperiodica".*

Key words: *galaxies—rotation and internal absorption.*

1. INTRODUCTION

The rotation curve $V(r)$ is the most important characteristic of disk galaxies. It not only provides information about the mass distribution but also allows empirical methods for determining the luminosity (distance) from the maximum rotation velocity to be used. For spiral galaxies with edge-on disks, constructing the rotation curve is nontrivial because of the following two complicating factors: projection and internal absorption. The two effects depend both on the shape of the rotation curve and on the distribution of the radiation sources and the absorbing medium in the galaxy.

The rotation curves or, to be more precise, one-dimensional line-of-sight velocity distributions over the disk were obtained for many edge-on galaxies. A distinctive feature of many of these galaxies is an extended region of rigid rotation (a monotonic increase in the velocity). A nearly linear increase in the line-of-sight velocity up to large galactocentric distances was pointed out in the first kinematic studies of galaxies with thin disks (Goad and Roberts 1981). These authors were, probably, the first to note that the rigidly rotating part of the rotation curve in edge-on galaxies could be an artifact and that the effects of a nonuniform dust distribution require drawing the envelope that bounds the positions of the data points in the radius–measured rotation velocity diagram from above. Bosma *et al.* (1992) clearly showed the effect of absorption on the shape of the rotation curve by comparing the optical and radio rotation curves for two edge-on galaxies (NGC 801 and NGC 100). As was shown by these authors using simple dust-containing disk models as an example, absorption rather than light scattering by dust affects the observed rotation-velocity estimates. They found that the absorption effect significantly decreases only if the disk orientation differs from the "edge-on" orientation by more than 5°.

Subsequently, a comparison of the shape of the rotation curve in the inner region with the disk inclination to the line of sight for a large number of galaxies confirmed that the gradient in the measured rotation velocity in the inner galaxy is actually lower for strongly inclined disks, and this effect is more pronounced for luminous galaxies, which, on average, exhibit stronger internal absorption (Giovanelli and Haynes 2002).

Curiously, at a sufficiently high optical depth, the effect of the diffuse dust medium on the mass estimate may prove to be significant not only for disk galaxies but also for slowly rotating (elliptical) galaxies (see Baes and Dejonghe (2000) and references therein).

More than 300 rotation curves for edge-on galaxies (from the Flat Galaxy Catalog (FGC) of Karachentsev *et al.* 1993) were obtained with the 6-m telescope at the Special Astrophysical Observatory of the Russian Academy of Sciences (see Makarov

*E-mail: zasov@sai.msu.ru

1063-7737/03/2907-0437$24.00

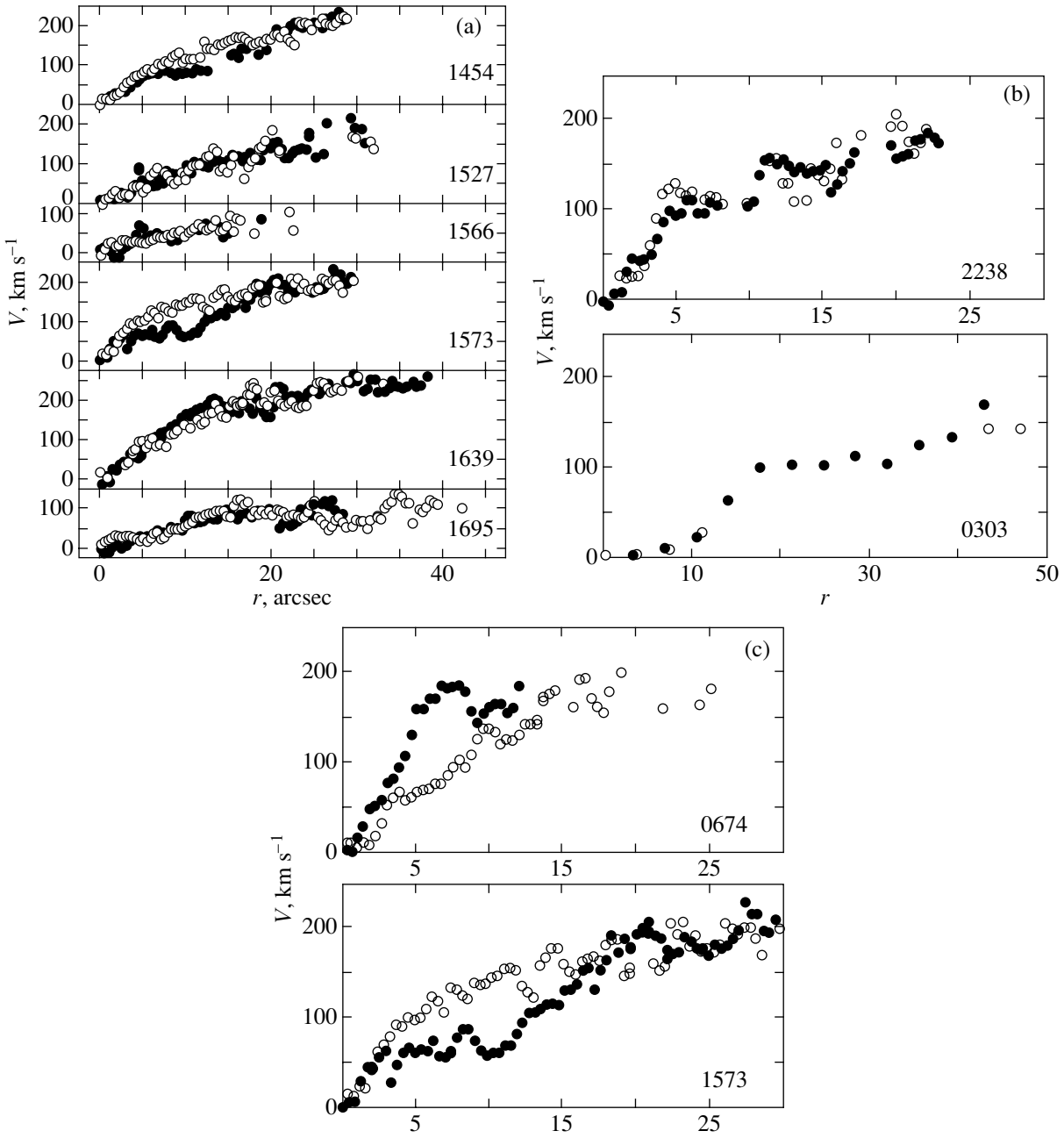

Fig. 1. Examples of the observed rotation curves for edge-on galaxies: (a) typical rotation curves; (b) examples of galaxies with a step on the rotation curve, and (c) examples of galaxies with different distributions of the measured velocities on different sides of the center. The filled and open circles correspond to the receding and approaching sides of the galaxy, respectively (Makarov *et al.* 1997, 1999; Karachentsev and Zhou Shu 1991). The galaxy number in the FGC catalog (Karachetnsev *et al.* 1993) is indicated.

et al. (2000) and references therein). The measurements confirmed that the overwhelming majority of these galaxies have an extended rigidly rotating portion, which occasionally extends to the outer boundary of the measured rotation curve, although there are exceptions (Makarov *et al.* 1997a, 1997b, 1999). As an example, Fig. 1a shows several typical rotation curves for galaxies from Makarov *et al.* 1997a). Figures 1b and 1c illustrate less common features of the rotation curves, which are discussed below (in Sections 2 and 3). The following questions arise in connection with the interpretation of the rotation curves: How do various effects affect the measured rotation velocities of such galaxies and can the actual rotation curve of the galaxy and an estimate of the

maximum disk rotation velocity be directly obtained from observations?

Here, for axisymmetric galaxy models with given rotation curves, we compute the line-of-sight velocity distributions $V_s(x)$ along the major axis of an edge-on disk under various assumptions about the spatial distribution of the gas (star) density—both in the absence and in the presence of internal absorption in the galaxy.

2. GALAXY MODELS

2.1. Absorption-Free Models

The case with low internal absorption can actually apply to rotation-velocity measurements in the radio wavelength range or in galaxies with a very low interstellar dust abundance, or to velocity measurements in the outer galaxy with a low optical depth τ.

In the absence of internal absorption, the maximum values of the Doppler rotation velocity component correspond to the regions located near the line perpendicular to the line of sight that crosses the galaxy along its diameter (we arbitrarily call it the major axis of the galaxy). Therefore, the maximum-velocity estimates for sources at a given galactocentric distance must represent (to within the velocity dispersion) the actual circular rotation velocity. However, in general, this velocity will not necessarily correspond to the centroid (barycenter) of the line profile, because its position depends on the distribution of not only the velocity but also the volume luminosity along the line of sight.

We assume that the rotation velocity of the disk, as well as its brightness in the spectral line used to measure the velocity, are distributed axisymmetrically. Denote the volume luminosity in the line by $S(r)$. Let the x axis correspond to the major axis of the galaxy and the y axis be directed along the line of sight (Fig. 2). The specific-luminosity-weighted mean velocity along the line of sight is then given by the expression

$$V_s(x) = \frac{\int\limits_{-y_0}^{y_0} S(r)V_\varphi(r)\dfrac{x}{\sqrt{x^2+y^2}}dy}{\int\limits_{-y_0}^{y_0} S(r)dy}, \qquad (1)$$

where R is the disk radius, $r = \sqrt{x^2+y^2}$, and the integration limit is $y_0 = \sqrt{R^2-x^2}$.

Since the models are axisymmetric, below we assume that the distance from the disk center in x projection is always positive.

Let us consider how the actual shape of the rotation curve $V_\varphi(r)$ and the peculiarities of the mass distribution in the disk affect the dependence $V_s(x)$ (the observed rotation curve).

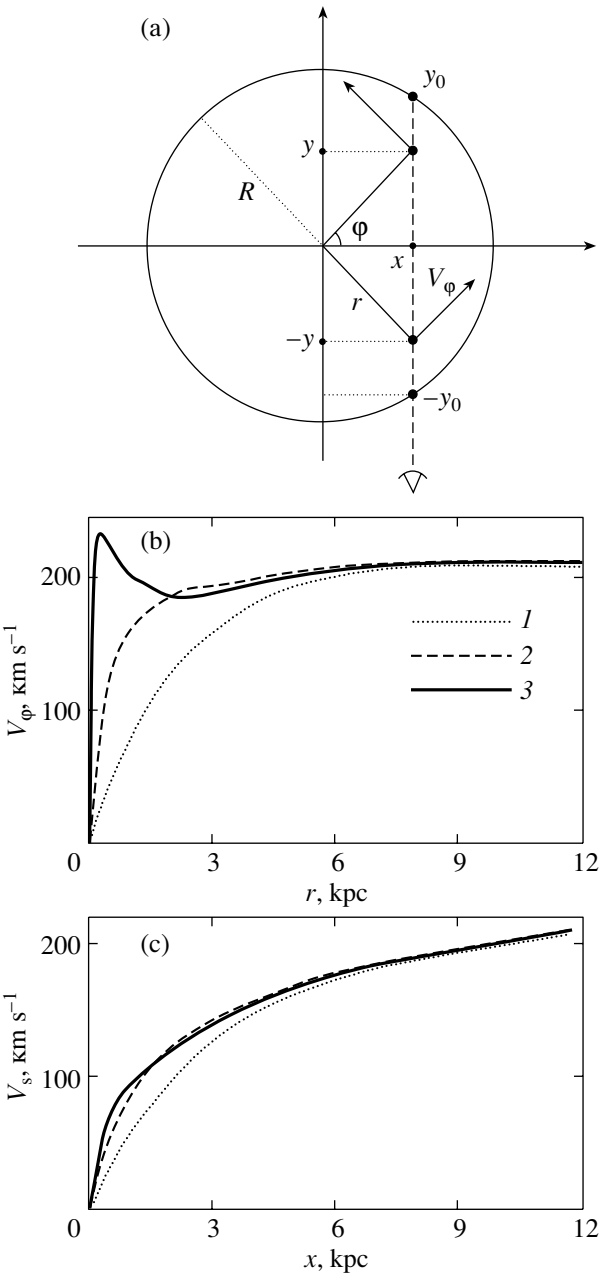

Fig. 2. (a) Determining the rotation velocity for an edge-on disk of radius R. At the point (x, y), the disk has the rotation velocity V_φ. The integration is performed from $-y_0$ to y_0. (b) The three types of rotation curves V_φ considered here (see also the text). (c) The line-of-sight velocity distribution relative to the center of the galaxy along its major axis $V_s(x)$ for the rotation curves shown in Fig. 2b with no allowance for internal absorption.

Let the disk volume luminosity in the spectral line used to estimate the velocity decrease exponentially with r:

$$S(r) = S_0 \exp(-r/L), \qquad (2)$$

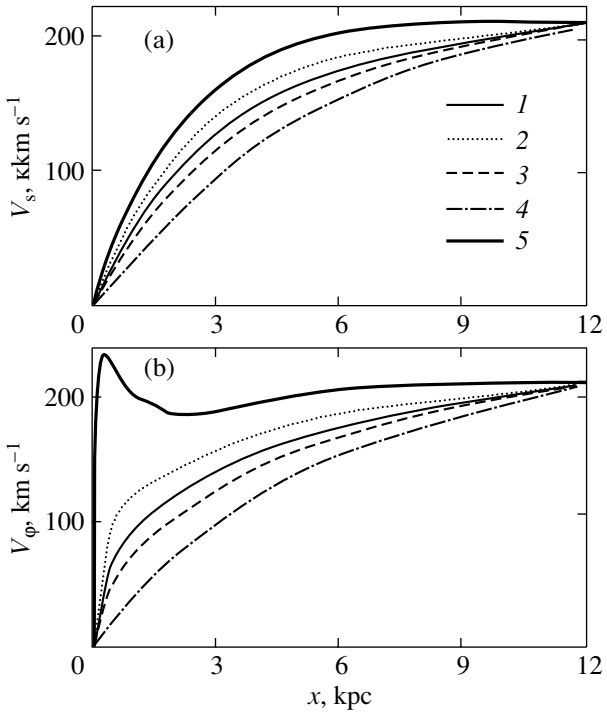

Fig. 3. The line-of-sight velocity distributions $V_s(x)$ for a gaseous disk with a chosen rotation curve (heavy lines). The models differ by the radial scale lengths L of the emission gas: *1*—$L = 3$ kpc, *2*—$L = 1.5$ kpc, *3*—$L = 6$ kpc, and *4*—$L = 6$ kpc with an allowance made for the central ring; (a) for the rotation curve V_φ of the first type (line *1* in Fig. 2b), (b) for the rotation curve V_φ of the third type (line *3* in Fig. 2b).

where L is the radial scale length of the disk brightness in the emission line or, in the case where the velocities are determined from absorption lines, the radial scale length of the stellar disk. We assume, for certainty, that $R = 4L$. The disk contribution to the observed line profile is assumed to be zero at galacticentric distances $r > R$. As an illustration, we restrict our analysis to the following three types of rotation curves with different shapes in the inner disk ($r \lesssim 2L$) (Fig. 2b):

(1) the rotation curve $V_{\varphi 1}$ typical of galaxies without massive bulges (the dotted line in Fig. 2b).

(2) the rotation curve of the second type $V_{\varphi 2}$ that takes place in the case of a low-mass bulge responsible for the steeper velocity gradient in the inner galaxy (the dashed line in Fig. 2b).

(3) the rotation curve $V_{\varphi 3}$ with a circumnuclear rotation-velocity maximum (the solid line in Fig. 2b) that reflects the existence of a massive concentrated bulge.

In all of these cases, the rotation curve flattens out at large r.

Figure 2c shows the radial dependences of the disk velocity along the line of sight $V_s(x)$ calculated using formula (1) for the three types of rotation curves under consideration in the absence of absorption. As we see, in all of these cases, the rotation velocity in the entire disk is significantly underestimated, particularly in the central region $r \lesssim 2L$. The difference between the curves of the first and second types virtually vanishes and the underestimation of the rotation velocity is largest for the rotation curve $V_{\varphi 3}$. Only at the very edge of the disk does the approximate equality $V_s \simeq V_\varphi$ holds. Since the velocity curves $V_s(x)$ depend only slightly on the actual shape of the rotation curve $V_\varphi(r)$, they do not allow the mass distribution in the galaxy to be reconstructed.

For any of the adopted dependences $V_\varphi(r)$, the velocity $V_s(x)$ increases with decreasing radial brightness scale length L in the spectral line, approaching $V_\varphi(r)$ (Figs. 3a and 3b). However, in general, the shape of the curve $V_s(x)$ weakly depends on L for any type of rotation curve.

The emission-gas distribution often appreciably deviates from an exponential one, particularly in the central region. In many spiral galaxies, gas forms a wide ring: the density exponentially decreases only at large r, while the central region exhibits a deficit of gas (Van den Bosch *et al.* 2000):

$$S(r) \propto r^\beta \exp\left(-r/L_{gas}\right), \qquad (3)$$

where the values of β lie within a wide range, $\beta = 0.2$–8 (Van den Bosch 2000).

The model with a gas ring at the radius of $r = L_{\rm gas}$ for $\beta = 1$ yields the observed rotation curve $V_s(x)$ shown in Figs. 3a and 3b (line *4*). The brightness decline in the central part of the galaxy causes an even more significant decrease in the measured $V_s(x)$. This effect is enhanced with increasing β. As a result, we can obtain a nearly linear dependence of the line-of-sight velocity for most of the disk.

2.2. Models with Absorption

When light passes through the disk matter, the contribution from the farther regions of the galaxy is smaller than the contribution from its regions located closer to the observer. As an illustration, Fig. 4 shows the lines of equal optical depth τ. Dust-containing galaxies are virtually opaque to the light that propagates in the disk at a small angle to its plane. Therefore, we can assume that the light from the farthest region A does not reach the observer. The light from the middle region B, where the line-of-sight rotation velocity is at a maximum, is significantly attenuated; the closer the center of the system, the stronger the absorption effect. As a result, in the central region of the galaxy ($r \lesssim R/2$), the nearest region C, in which the line-of-sight velocity is low, mainly contributes to

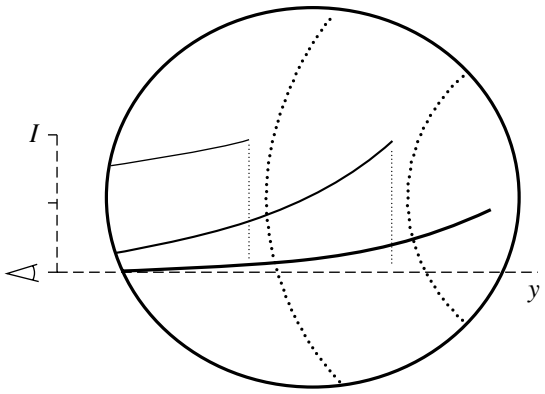

Fig. 4. A scheme that shows the effect of internal absorption in the galaxy on the measured rotation velocity.

the light. When corrected for absorption, relation (1) takes the form

$$V_s(x) = \frac{\int\limits_{-y_0}^{y_0} S(r)\exp(-\tau(x,y))V_\varphi(r)\dfrac{x}{\sqrt{x^2+y^2}}dy}{\int\limits_{-y_0}^{y_0} S(r)\exp(-\tau(x,y))dy}, \quad (4)$$

where the quantity $\tau(x,y)$, which characterizes the optical depth per unit length in the disk plane, is determined by the dust distribution function $f_{\rm dust}(x,y)$:

$$\tau = \int\limits_{y_0}^{y} f_{\rm dust}\,(x,\xi)\,d\xi. \quad (5)$$

For simplicity, we restrict our analysis to an axisymmetric exponential dust distribution:

$$f_{\rm dust}(x,y) = \alpha_d \exp\left(-\frac{\sqrt{x^2+\xi^2}}{L_d},\right) \quad (6)$$

where $L_{\rm d}$ is the radial scale length of the distribution of the absorbing medium and $\alpha_{\rm d}$ is the normalization parameter. Following the gas-density distribution, the function $\tau(x)$ decreases with galactocentric distance and becomes zero at $r = R$. Let us define the parameter $\tau_0(x)$ as the optical depth per unit length (1 kpc) on the major axis of the galaxy at the galactocentric distance $r = x$. Being proportional to $f_{\rm dust}$, this quantity reflects the density of the absorbing medium at a given galactocentric distance x. When we constructed the model dependences of the line-of-sight velocity along the galactic disk, we varied the parameter $\alpha_{\rm d}$ between 0 and 6, which corresponds to a variation of the optical depth τ_0 between 0 and 2.2 kpc^{-1} at the galactocentric distance $x = 3$ kpc.[1]

[1]The opacity in units of τ kpc^{-1} roughly corresponds to the attenuation in magnitudes per 1 kpc.

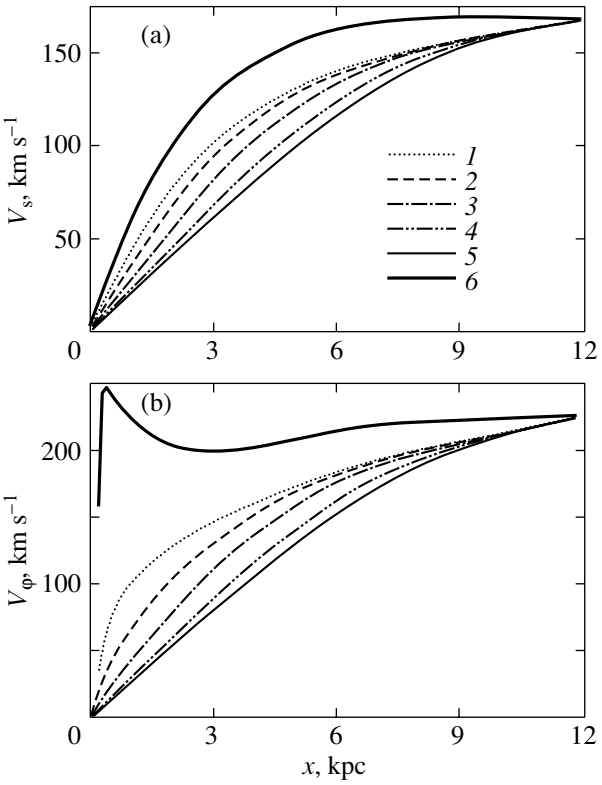

Fig. 5. The absorption-corrected line-of-sight velocity distributions $V_s(x)$ for the radial scale length of the dust distribution $L = L_{\rm d} = 3$ kpc. (a) The dependences $V_\varphi(r)$ (a bulgeless model) and $V_s(x)$ for various optical depths at $r = 3$ kpc: *1*—$\tau_0 = 0$ kpc^{-1}, *2*—$\tau_0 = 0.37$ kpc^{-1}, *3*—$\tau_0 = 0.73$ kpc^{-1}, *4*—$\tau_0 = 1.46$ kpc^{-1}, and *5*—$\tau_0 = 2.2$ kpc^{-1}. (b) The same for the rotation curve of the third type (see Fig. 2b).

Figure 5 shows the results of our calculations using formula (4) with an allowance made for relations (2), (5), and (6) for the radial scale lengths of the distributions of the emission-line brightness and the dust density equal to $L = 3$ kpc and $L_{\rm d} = 3$ kpc, respectively, at various values of τ_0. In all cases, the absorption greatly decreases the velocity $V_s(x)$, except for the outer, relatively transparent part of the galaxy. As a result, the observed rotation curve straightens out. Therefore, in a very dusty disk, a nearly linear increase in $V_s(x)$ can be traced up to the outer disk boundary, irrespective of the actual shape of the rotation curve (see Fig. 5). The presence of a ring and a central hole (see formula (3)) in the gas distribution enhances this feature in the behavior of the curve $V_s(x)$ even further in models with absorption.

3. EFFECTS OF RANDOM MOTIONS

3.1. The Model

In the models considered above, we assumed that the velocity dispersion of the radiation sources was

equal to zero and that there was only regular rotation. Let us now take into account the residual velocities, which we will characterize by the dispersions of the radial (c_r) and azimuthal (c_φ) velocities. If the rotation curve is estimated from stellar spectra, then we can assume, in accordance with observations (see, e.g., Bottema 1993), that both c_r and c_φ decrease with increasing galactocentric distance. For c_r, we adopt the simple expression

$$c_r = c_{r0}\exp(-r/L_c). \quad (7)$$

As a rule, the radial scale length L_c of the velocity dispersion is several times larger than the density scale length L. We choose a velocity distribution function in the form

$$F = F_0\exp\left\{-\frac{(V_\varphi - v_\varphi)^2}{2c_\varphi^2} - \frac{v_r^2}{2c_r^2}\right\}, \quad (8)$$

where c_r and c_φ are the velocity dispersions for the random velocity components v_r and v_φ, respectively. The line profile, which reflects the velocity variation along the line of sight, at a fixed observed distance from the center of the galactic disk is given by the expression

$$I(v_y, x) = I_0\int\limits_{-y_0}^{y_0} S(x,y)\exp(-\tau)F(x,y,v_y)dy, \quad (9)$$

where I_0 is the normalization constant and τ is determined by integral (5).

3.2. The Observed Rotation Curves for Gaseous and Stellar Disks

Let us consider separately the effects of the factors described above on the observed rotation curves of the dynamically hot (stellar disk) and cold (gaseous disk) subsystems for edge-on galaxies. For the gaseous disk, $c_r/V_{\max} \ll 1$ (where $V_{\max}$ is the maximum rotation velocity) and the velocity distribution is isotropic ($c_r = c_\varphi$). Figure 6 shows the velocity profiles (Doppler line profiles) $I(V) = I(v_y, x)$ at various distances from the disk center. In the absence of dust (Fig. 6a), the profiles differ greatly for different distances x. A characteristic feature of the profiles is their asymmetry and, for the central region (curves *1*–*3* in Fig. 6a), the presence of two peaks or a long wing with a "step" in place of the second peak (curves *4*–*7*). The first peak (at high velocities) is attributable to the rapid rotation of the matter in the region $|\varphi| \ll 1$ near the "major axis" (see Fig. 2a). The second peak or the step (at lower velocities) is associated with two factors: the presence of residual velocities, but, to a greater extent, the large decrease in the line-of-sight velocity component V_φ at $|\varphi| > \pi/4$.

The situation qualitatively changes in a very dusty disk (Fig. 6b). All $I(V)$ profiles in the central region exhibit only one peak (of the two peaks observed in the previous case, only the peak that corresponds to a lower velocity remains). The peak at a higher velocity emerges only when the absorption is low enough to make it possible to observe the regions near the major axis at a given distance x.

The velocity dispersion for the stellar disk is higher than that for the gas. For an axisymmetric model, $c_\varphi = \dfrac{\partial e}{2\Omega}c_r$, where the epicyclic frequency ∂e and the angular velocity Ω can be calculated from the dependence $V_\varphi(r)$. Figures 6c and 6d show the distributions $I(V)$ for a stellar disk with a central stellar radial velocity dispersion $c_r(0)/V_{\max} = 0.5$ (where $I(V)$ is taken in absolute value, because we deal with absorption lines). In this case, as in the case of emission gas, the $I(V)$ peaks shift toward lower velocities in the presence of absorption.

The complex shape of the line profiles results in a difference between the line-of-sight velocities estimated from the measurement of the wavelengths that correspond to the intensity peak and the wavelengths of the line "barycenter." Figure 7 shows the dependences $V_\varphi(r)$ and $V_s(x)$ constructed from the positions of the peaks in the $I(V)$ profiles shown in Figs. 6a–6d. According to what was said above, in the presence of two peaks, we chose the peak at a higher velocity. In the model of an absorption-free gaseous disk (Fig. 6a), this method of estimating the velocity yields a small difference between the actual rotation velocity V_φ and $V_s(x)$ (curves 1 and 2 in Fig. 7). In our case, it does not exceed 7% (see Fig. 7).

The difference $V_\varphi - V_s(x)$ is much higher for a stellar population with a large velocity dispersion, $c_r(0)/V_{\max} = 0.5$. However, in this case, the internal peak is also clearly traceable in the rotation curve (curve *3*), although its amplitude is appreciably smaller.

Thus, the approach based on the determination of the $I(V)$ peak yields a more accurate result when constructing the rotation curve than does the method of the weighted mean line-of-sight velocity determined from the line "barycenter" (see Section 2). Unfortunately, obtaining the shape of the line profile with an accuracy sufficient for a detailed comparison with the model profiles presented here requires a spectral resolution that is difficult to achieve. Besides, the line profiles in real galaxies are usually distorted by the nonuniform distribution of the emission regions and the absorbing medium. However, the asymmetry of the profile, if present, can be measured and taken into account when estimating the velocity.

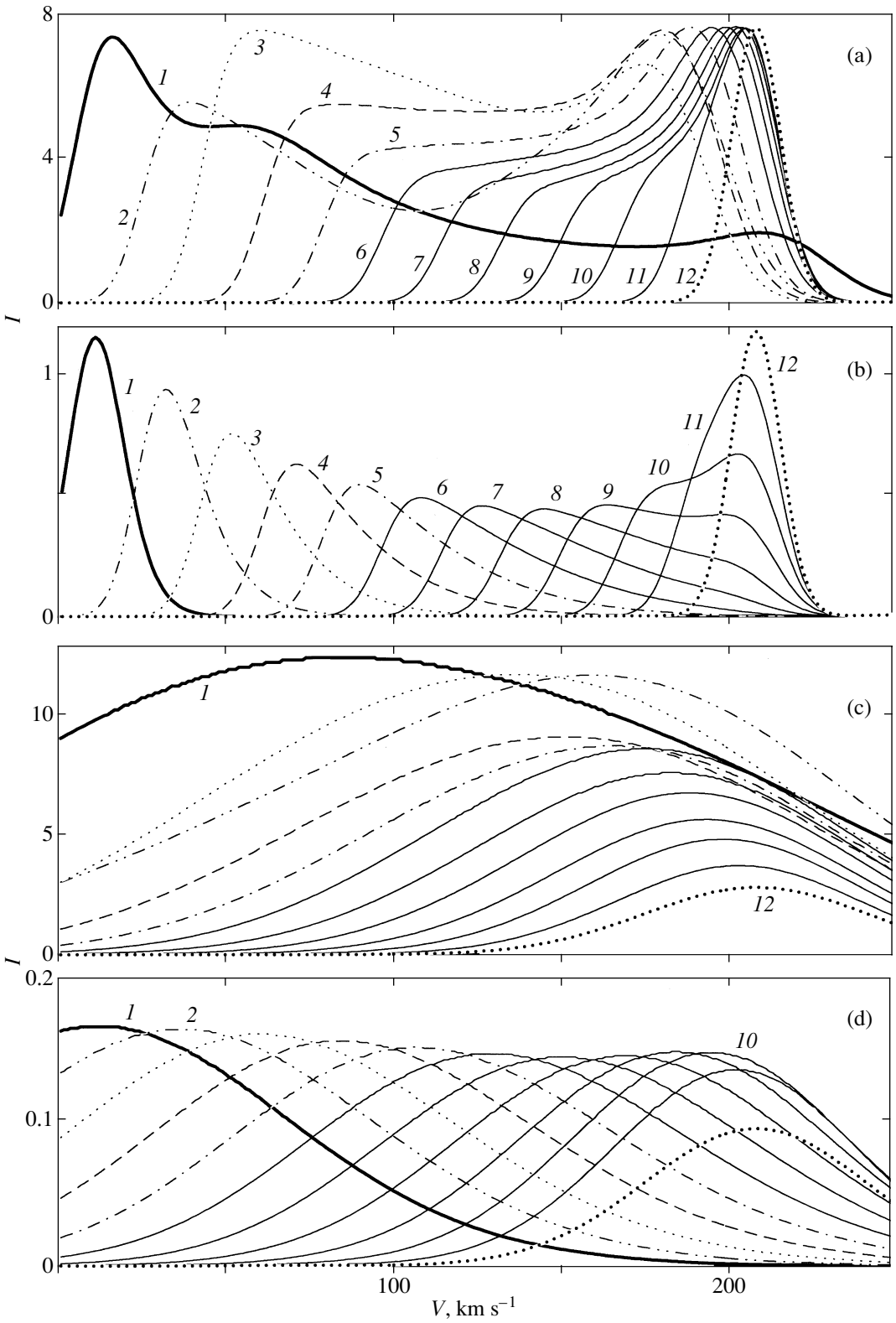

Fig. 6. (a) The line profiles $I(V)$ at various galactocentric distances for a model gaseous disk with the velocity dispersion $c_r(0) = 15$ km s^{-1} and the radial scale length $L_c = 9$ kpc (with no allowance for absorption). The functions $I(V)$ are normalized arbitrarily. The disk is broken down into 12 zones; the numbers indicate the zone numbers in order of increasing distance from the disk center. (b) The same for the model of a very dusty disk with $\tau_0 = 2.2$ kpc^{-1}. (c) The same for the model of an absorption-free stellar disk with $c_r(0) = 100$ km s^{-1}, $L_c = 3$ kpc. (d) The same for the model of a very dusty disk with $\tau_0 = 2.2$ kpc^{-1}.

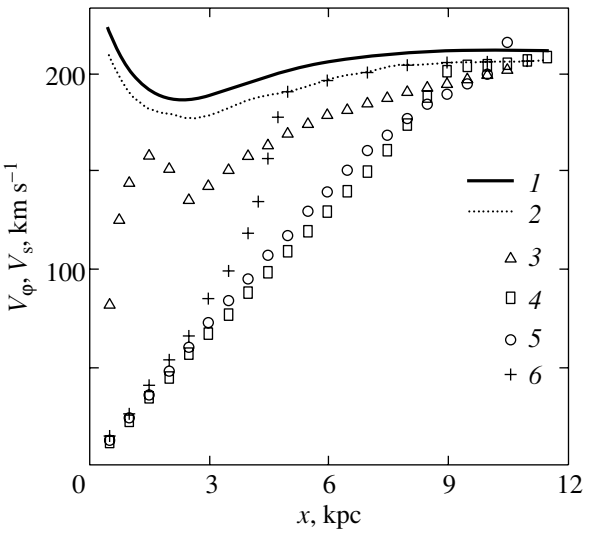

Fig. 7. The specified galactic rotation curve ($V_\varphi(r)$, curve *1*) in comparison with the measured rotation velocities $V_s(x)$ constructed from the maxima of the function $I(V)$ (see the text) for the following models: *2*—an absorption-free gaseous disk; *3*—an absorption-free stellar disk; *4*—a gaseous disk with strong absorption ($\tau_0 = 2.2$ kpc^{-1}); *5*—a stellar disk with strong absorption ($\tau_0 = 2.2$ kpc^{-1}), and *6*—a gaseous disk with weak absorption ($\tau_0 = 0.73$ kpc^{-1}). In all cases, the radial scale length of the gas and dust distribution was assumed to be 3 kpc, and τ_0 refers to 3 kpc.

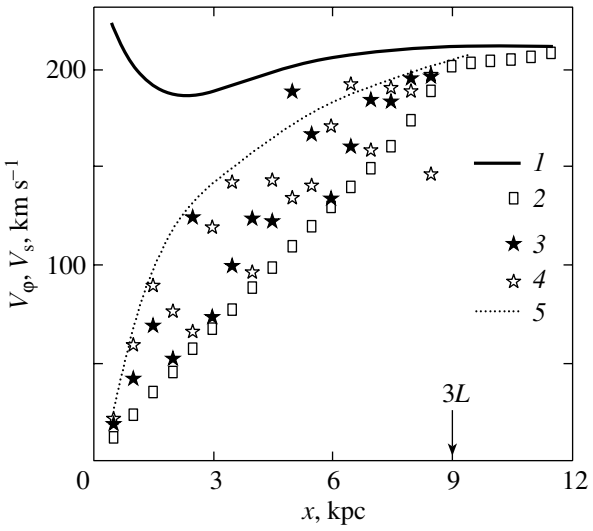

Fig. 8. The radial profile of the actual rotation velocity for a model galaxy (V_φ, curve *1*) and the measured velocities for an edge-on galaxy (the same as Fig. 7) for the following models: *2*—a gaseous disk with strong absorption and a smooth dust distribution; *3* and *4*—a disk with the same parameters and a random distribution of absorbing regions (the filled and open symbols refer to the two halves of the disk), and *5*—a fitting curve.

In a very dusty disk, the dependences $V_s(x)$ derived by the two methods differ little for the gaseous and stellar populations (Fig. 7). In both cases, the inferred rotation curve $V_s(x)$ does not give a correct idea of the shape of the actual rotation curve in the inner disk.

Of greatest interest is the intermediate case where the absorption is strong in the central region of the galaxy (the line profile exhibits only one peak, at low velocities), and, starting from some value of x, the regions near the major axis that are responsible for the high-velocity peak significantly contribute to the observed radiation. In this case, the rotation curve constructed from the positions of the peaks in the line profiles exhibits a sharp "jump" from velocities much lower that the rotation velocity to velocities close to the latter (curve 6 in Fig. 7). The weaker is the absorption in the galaxy, the closer to the center this transition occurs. By varying τ_0 in the models under consideration, we found that the rise in the measured rotation velocity occurs at a radius r at which the absorption drops below $0.3{-}0.5^m$ per 1 kpc. Such a step in the rotation curve is actually observed in several edge-on galaxies (see the example in Fig. 1b).

The calculations described in Subsections 3.2 and 3.3 refer to the rotation curve $V_{\varphi,3}$ (see Fig. 2b). The main conclusions remain valid for the cases $V_{\varphi,2}$ and $V_{\varphi,1}$.

3.3. Models with a Nonuniform Dust Distribution

As observations indicate, the dust distribution in the disks of galaxies is highly asymmetric and nonunofirm on small scales ($\ll L$). As an illustration, let us consider a model in which the absorbing regions are distributed by "spots" randomly scattered over the disk. We will characterize the concentration of dust in the ith cloud ($i = 1, ..., m$) with central coordinates $(x_\mathrm{d}^{(i)}, y_\mathrm{d}^{(i)})$ by the quantity $\tau^{(i)}$, which obeys law (6). In this model, the cloud sizes $l_\mathrm{d}^{(i)}$ were specified randomly from the interval $0.1L \le l_\mathrm{d}^{(i)} \le 0.5L$.

Figure 8 shows the radial dependence of the velocity $V_s(x)$ in the model with $m = 50$ and $\tau_0 = 2.2$ (curves *3* and *4*). Clearly, the scatter of points or the irregular shape of the curve $V_s(x)$, which is asymmetric relative to the center of the galaxy, result from the existence of randomly located transparency corridors, which allow the regions located deep in the disk to be observed in some directions. The amplitude of the velocity variations can be significant, and, as was suggested by Goad and Roberts (1981), to obtain the rotation curve, we must draw the upper envelope of the points in the $V_s(x)$ diagram. However, even in this case, the shape of the rotation curve to be traced only approximately. If the mean dust density is sufficiently low, so that we observe the regions located near the major axis at different distances x, the above procedure actually makes it possible to obtain the

rotation curve. However, this is most likely true for the outer regions of the galaxy where τ_0 is small. For the model under consideration, even the envelope of the data points in the $V_s - r$ diagram (the dotted line in Fig. 8) is far from the specified shape of the rotation curve.

It would be natural to expect another effect produced by a nonuniform dust distribution for galaxies with a well-developed spiral structure. A certain orientation of the spiral arms toward which the interstellar medium concentrates leads to different disk transparencies on different sides of the center. Where the spiral arm is located on the side of the galaxy facing the observer, the line of sight penetrates the disk to a smaller depth, which decreases the rotation-velocity estimate. As a result, the measured curves $V_s(x)$ are asymmetric relative to the center. Such cases are actually observed (see Fig. 1c). The curve drawn through higher measured velocities should be considered to be closer to the actual shape of the rotation curve.

At large x, all of the observed rotation curves ($V_s(x)$) in the models considered in this and previous sections flatten out , which corresponds to the specified rotation velocity of the model galaxy. Therefore, the measured maximum rotation velocities of edge-on disks must differ little from the actual values.

4. DISCUSSION AND CONCLUSIONS

Simple axisymmetric disk models for edge-on galaxies clearly show that the effects of geometrical projection, internal absorption, and velocity dispersion are the factors that can irreparably distort the observed shape of the rotation curve, particularly in the inner galaxy, making it similar to the shape imitating rigid rotation. For this reason, the rotation curves with a large velocity gradient in the central region undergo the greatest distortion, while the rotation curves of low-mass galaxies, which usually monotonically rise to the optical disk boundaries, undergo the smallest distortion. That is why in many cases, the observed rotation curves of edge-on galaxies rise almost linearly out to the peripheral disk regions.

The errors in the measured velocities of the stellar disk (as estimated from absorption lines) increase appreciably due to the higher (than for the gas) velocity dispersion of the disk stars. For the central region of the galaxy, the error in the estimated velocity can be 20–50% even in the absence of absorption.

The projection effect, as well as the absorption effect, tends to straighten out the observed rotation curve. However, its role can be significantly reduced if the velocity at a given galactocentric distance is measured from the position of the high-velocity peak (or the high-velocity cutoff) in the line profile rather than from its centroid. In this case, in the absence of absorption, the actual shape of the rotation curve of the galaxy can be accurately reproduced from observations even for the inner disk. This method of measurement may be applied to lenticular galaxies with a low dust content and to galaxies whose rotation curves are constructed from radio observations.[2]

Unfortunately, the low intensity of the emission and the nonuniform distribution of the emission regions and the absorbing medium make it difficult to measure the shapes of the optical line profiles for actual edge-on galaxies with spectral and spatial resolutions that would allow detailed comparisons with model profiles. However, the asymmetry or the double-peaked line profiles for regions with moderate absorption that follows from the models can be found and taken into account when analyzing the observed rotation curve (see Subsection 3.2).

Strong internal absorption in the disk qualitatively changes the situation. As the models show, the two methods of measuring the velocity (from the position of the line peak and centroid) yield a monotonically (almost linearly) rising $V_s(x)$ curve up to galactocentric distances of several radial brightness scale lengths L. The double-peaked pattern of the line profiles disappears. This effect is only enhanced if there is a deficit of gas in the central region of the galaxy. The actual shape of the rotation curve in the opaque disk region can no longer be reconstructed from observations without using additional data. The transition from underestimated to actual rotation velocities occurs at a galactocentric distance where the absorption is equal to several tenths of a magnitude per 1 kpc. In this case, the observed rotation curve can exhibit a step, which is actually observed in some galaxies (see Subsection 3.2).

Curiously, contrary to the expectations, the line-of-sight velocity curves $V_s(x)$ for some edge-on galaxies exhibit no rigid rotation. In these galaxies, the central region is characterized by a high line-of-sight velocity gradient (Fig. 1c). Such a behavior implies either a very low dust content in the galaxy or (more likely) a significant deviation of the disk inclination from $i = 90°$. A deviation of several degrees can be enough for the effects of projection and internal absorption to become negligible (the accurate estimate of this angle depends on the disk thickness and on the spatial distribution of the radiation sources and the absorbing medium). The projection effect depends not only on the disk inclination i but also on the

[2]This approach is similar to the method for constructing the rotation curve by drawing the envelope in the position–velocity diagram based on radio observations (the envelope-tracing method) (Sofue 1996).

spectrograph slit width. Thus, if the slit is along the major axis of the galaxy and if its width is comparable to the apparent disk thickness (more precisely, to the size of the minor axis of the ellipse that bounds the disk region being measured), then the disk will be perceived as seen edge-on even if its inclination differs from 90°.

To summarize, note that although the shapes of the rotation curves of edge-on galaxies are generally of little use in estimating the masses of the individual components (particularly for galaxies with steep central gradients in rotation velocity), their analysis can yield a correct estimate of the rotation velocities for the outer disk regions and, consequently, a rough estimate of the total mass within a sufficiently large radius. In some cases, analysis of the observed rotation curve can provide information about the distribution of the absorbing medium in the galaxy.

ACKNOWLEDGMENTS

We are grateful to D. I. Makarov for useful discussions and help in choosing the illustrations of the galactic rotation curves. This work was supported by the Russian Foundation for Basic Research (project no. 01-02-17597) and, in part, by the Federal Science and Technology Program "Research and Development in Priority Fields of Science and Technology" (contract no. 40.022.1.1.1101 юf February 1, 2002).

REFERENCES

1. M. Baes and H. Dejonghe, Mon. Not. R. Astron. Soc. **335**, 441 (2002).
2. R. Bottema, Astron. Astrophys. **275**, 16 (1993).
3. F. C.van den Bosch, J. J. Robertson, and J. J. Dalcanton, Astron. J. **119**, 1579 (2000).
4. A. Bosma, Y. Byun, K. C. Freeman, and E. Athamassoula, Astrophys. J. **400**, L 21 (1992).
5. J. W. Goad and M. S. Roberts, Astrophys. J. **250**, 79 (1981).
6. R. Giovanelli and M. P. Haynes, Astrophys. J. **571**, L107 (2002).
7. I. D. Karachentsev and Zhou Shu, Pis'ma Astron. Zh. **17**, 321 (1991) [Sov. Astron. Lett. **17**, 135 (1991)].
8. I. D. Karachentsev, V. E. Karachentseva, and S. L. Parnovsky, Astron. Nachr. **313**, 97 (1993).
9. D. I. Makarov, A. N. Burenkov, and N. V. Tyurina, Pis'ma Astron. Zh. **25**, 813 (1999) [Astron. Lett. **25**, 706 (1999)].
10. D. I. Makarov, I. D. Karachentsev, and A. N. Burenkov, astro-ph/0006158 (2000).
11. D. I. Makarov, I. D. Karachentsev, A. N. Burenkov, *et al.*, Pis'ma Astron. Zh. **23**, 734 (1997) [Astron. Lett. **23**, 638 (1997)].
12. D. I. Makarov, I. D. Karachentsev, N. V. Tyurina, and S. S. Kaisin, Pis'ma Astron. Zh. **23**, 509 (1997) [Astron. Lett. **23**, 445 (1997)].
13. Y. Sofue, Astrophys. J. **458**, 120 (1996).

Translated by A. Dambis